Effects of Cell Construction Parameters on the Performance of Lithium/Sulfur Cells

Min-Kyu Song
The Molecular Foundry, Lawrence Berkeley National Laboratory, Berkeley, CA 94720

Dept. of Chemical and Biomolecular Engineering, University of California, Berkeley, CA 94720

Yuegang Zhang
The Molecular Foundry, Lawrence Berkeley National Laboratory, Berkeley, CA 94720

Elton J. Cairns
Dept. of Chemical and Biomolecular Engineering, University of California, Berkeley, CA 94720

Environmental Energy Technologies Division, Lawrence Berkeley National Laboratory, Berkeley, CA 94720

DOI 10.1002/aic.14947
Published online August 7, 2015 in Wiley Online Library (wileyonlinelibrary.com)

Current lithium-ion batteries are predicted to be unable to provide the specific energy required to meet the ever-increasing demands of rapidly emerging technologies. Due to a high theoretical specific capacity of 1675 mAh/g, sulfur has gained much attention as a promising positive electrode material for high specific energy rechargeable batteries. Although the lithium/sulfur cell has been studied for many years and continues to receive much attention today as an alternative power source for zero-emission vehicles and advanced electronic devices, the realization of this novel cell's promise as a commercial product has yet to be successful. The major problems with sulfur electrodes involve: (1) the dissolution of sulfur (as polysulfides) and the resulting diffusion of dissolved polysulfides and (2) the deposition of insulating products (including Li_2S) on both the negative and the positive electrodes. These solid deposits can physically block the electrode reaction sites, thus passivating the electrode surfaces. Another important problem is the large volume change that occurs with the conversion of S to Li_2S. It is important to understand that the performance of Li/S cells is hampered by linked chemical and mechanical degradations and both degradation mechanisms must be correctly alleviated in order to markedly improve current-technology Li/S cells. In this study, improved cycling performance via the reactive functional groups on graphene oxide to successfully immobilize sulfur and lithium polysulfides during operation has been demonstrated. The use of a new electrolyte and binder leads to improved cell performance in terms of high-rate capability (up to at least 2 C) and good reversibility ($S \leftrightarrow Li_2S$), yielding at least 800 cycles have also been demonstrated. © 2015 American Institute of Chemical Engineers *AIChE J*, 61: 2749–2756, 2015
Keywords: sulfur, graphene oxide, nanocomposites, electrolyte, binder, lithium batteries

Introduction

Among electrochemical energy storage devices, rechargeable lithium-ion batteries still embody the state-of-the-art technology available in the present market.[1–3] However, there are several challenges that continue to require attention.[4] Above all, it is believed that current oxide-based cathode materials have insufficient capacity to meet the important needs of emerging technologies such as electric vehicles or plug-in hybrid electric vehicles.[5,6] Advanced batteries with a capability of more than 400 Wh/kg are desired because current lithium-ion batteries are reaching their maximum specific energy (~225 Wh/kg).[7,8] Recently, lithium/sulfur cells, with a theoretical specific energy of 2680 Wh/kg, have emerged as a promising candidate for a new power source for electric vehicles and advanced electronic devices.[9–21] The very high theoretical specific capacity (1675 mAh/g) of sulfur electrodes, based on a two-electron reaction, is notably larger than that of current cathode materials.

Sulfur cathodes, however, have shown a short cycle life and poor rate capability that has previously restricted further development of this attractive technology into a practical product.[22–26] When sulfur atoms electrochemically react with lithium ions to form Li_2S, intermediate lithium polysulfide species are produced and they are readily soluble in most organic electrolytes. This indicates that active materials are lost from the positive electrode during cell operation, which is a major reason for the poor cycling performance. In addition to the loss of sulfur, the dissolved lithium polysulfides can diffuse to the

Correspondence concerning this article should be addressed to E. J. Cairns at ejcairns@lbl.gov.

Current address of Y. Z.: *i-LAB*, Suzhou Institute of Nano-Tech and Nano-Bionics, Chinese Academy of Sciences, Suzhou, 215123, China.

© 2015 American Institute of Chemical Engineers

lithium metal anode.[27] Lithium metal, if not suitably protected, has high reactivity with these polysulfides, therefore, a solid precipitate of Li_2S can form on the surface of the lithium metal electrode, increasing the cell resistance and lowering the coulombic efficiency. Additionally, the conversion reaction between sulfur and Li_2S involves an approximate 76% volume change (expansion/contraction), which can result in the mechanical degradation of the sulfur electrode upon cycling.

It is crucial to understand that this polysulfide shuttling involves not only the sulfur electrode but also the lithium electrode and the electrolyte.[12] These degradation mechanisms need to be properly mitigated in order to realize the potential of this promising technology. More comprehensive research is urgently required to solve the problems associated with these complex, interrelated processes in order to dramatically increase the cycle life of lithium/sulfur cells and to improve their performance overall. In the literature, many interesting approaches have been explored,[17,28–31] with some success, to develop improved lithium/sulfur cells. As yet, however, it is not clear how to design the most advantageous electrode structures and electrolytes to attain optimal performance.

Here, we report that the performance of lithium/sulfur cells can be significantly improved by modifying the active material structure, electrolyte, and binder. For the sulfur electrode, graphene oxide (GO) with various surface functional groups was used as a component of the nanostructured composite S–GO electrode material. With the help of these functional groups as well as an ionic liquid-based electrolyte and an elastomeric binder, the sulfur can be retained during cell cycling. Even after 800 cycles, we demonstrated a very high specific capacity of ~787 mAh/g of sulfur.

Experimental Section

An amount of 0.58 g of sodium sulfide (Na_2S, anhydrous, Alfa Aesar) was dissolved in 25 mL ultrapure water (Millipore) to form a Na_2S solution. An amount of 0.72 g of elemental sulfur (S, sublimed, 99.9%, Mallinckrodt) was then added to the Na_2S solution and was stirred for 2 h with a magnetic stirrer to obtain a sodium polysulfide (Na_2S_x) solution. Commercial GO–water dispersion (10 mg/mL, ACS Material) was used to form a GO suspension (180 mg of GO in 180 mL of ultrapure water). Different amounts (9 and 328 mg) of cetyltrimethyl ammonium bromide (CTAB, $CH_3(CH_2)_{15}$ N(Br) $(CH_3)_3$, Sigma Aldrich) were added to the GO suspension and stirred for 2 h. The Na_2S_x solution was added to the prepared GO-CTAB-blended solution dropwise while stirring. Then, the Na_2S_x–GO-CTAB blended solution was stirred overnight. The Na_2S_x–GO-CTAB-blended solution was slowly added to 100 mL of 2M formic acid (HCOOH, 88%, Aldrich) using a burette while stirring. The resulting mixture was stirred for 2 h to allow for sulfur to be deposited onto the GO. Lastly, the CTAB-modified S-GO composite was filtered and washed with acetone and ultrapure water several times to remove any salts and impurities. Then, the CTAB-modified S-GO composite was dried at 50°C in a vacuum oven for 24 h, followed by heat-treatment at 155°C for 12 h under a flowing argon atmosphere (100 cc/m) in a tube furnace. A scanning electron microscope (SEM, Zeiss Gemini Ultra-55) was used with an accelerating voltage of 3 kV to observe the morphology of the CTAB-modified S-GO nanocomposite. An energy dispersive x-ray spectrometer attached to the SEM (JEOL JSM-7500F) was operated at an accelerating voltage of 10 kV to perform elemental analysis of sulfur and its distribution. Thermogravimetric analysis (TGA, TA Instruments Q5000) was used to determine the weight of the S on the GO using a heating rate of 10°C/min in N_2.

The sulfur electrodes were fabricated by mixing the S-GO nanocomposite, carbon black (Super C65) with a binder, either polyvinylidene fluoride (PVDF) or styrene butadiene rubber (SBR)/carboxymethyl cellulose (CMC) 1:1 by weight, at a weight ratio of 70:20:10 in *N*-methyl-2-pyrrolidone solvent for PVDF or ethanol/water solution for SBR/CMC to form slurry using an ultrasonicator. The resulting slurry was spread using a doctor blade (Elcometer 3540 Bird Film Applicator) on pure aluminum foil. The solvent was allowed to evaporate at room temperature for 24 h before the electrodes were dried in a vacuum oven at 50°C for 48 h. The electrode was cut into circular pieces with a diameter of 12.7 mm for cell assembly. The average sulfur loading of the electrodes was ~0.6 mg/cm^2 and the thickness of sulfur electrode is estimated to be 20–30 μm. For the electrolyte, 1 mol/kg lithium *bis*(trifluoromethylsulfonyl)imide (LiTFSI, Sigma-Aldrich) in (*n*-methyl-(*n*-butyl) pyrrolidinium *bis*(trifluoromethanesulfonyl)imide (PYR_{14} TFSI, Sigma-Aldrich)/polyethylene glycol dimethyl ether (PEGDME, Sigma-Aldrich) mixture (1:1, by volume) was prepared and used for evaluation of the electrochemical performance of electrodes with different sulfur loadings, CTAB amounts, and heat treatments. For the long-term cycling tests and rate capability measurements, a mixture of 1,3-dioxolane (DOL) and dimethoxyethane (DME) was introduced to PYR_{14}TFSI to form 1M LiTFSI in PYR_{14}TFSI/DOL/DME mixture (2:1:1 by volume). $LiNO_3$ (0.1M) was used as an additive in the electrolyte. CR2035-type coin cells were assembled by sandwiching two separators (Celgard 2400) between a lithium metal foil (99.98%, Cyprus Foote Mineral) and a sulfur electrode fabricated with the S-GO composite in an argon-filled glove box. Constant-current discharge and charge testing of the coin cells was performed using a battery cycler (Maccor Series 4000) at different rates between 1.5 (or 1.7) and 2.8 V. The cell capacity was normalized both by the weight of sulfur and the total electrode mixture weight. Before all electrochemical characterizations, the cells were held at open circuit at room temperature for 24 h. All electrochemical characterizations were performed inside a chamber (TestEquity TEC1) maintained at 30°C.

Results and Discussion

Synthesis and characterization of CTAB-modified S-GO nanocomposites

To achieve high electrochemical utilization of sulfur, it is important to uniformly deposit the poorly conducting sulfur on the conductive GO.[12] Additionally, porous substrates can help minimize the loss of sulfur. In addition to the physical absorption approach, GOs can act as a sulfur immobilizer because oxygen-containing functional groups on the surface of GO weakly bind to sulfur and polysulfides during cell operation.[31,32] In this study, sulfur was deposited onto GO using a simple, aqueous solution-based precipitation method by acidifying the sodium polysulfides in formic acid in the presence of CTAB and GO in water, followed by heat-treatment under an argon atmosphere at 155°C. The morphologies and some characterization results for the S-GO nanocomposite synthesized with different amounts of CTAB are shown in Figures 1 and 2. SEM images shown in Figures 1a and 2a reveal the typical morphology of the S-GO

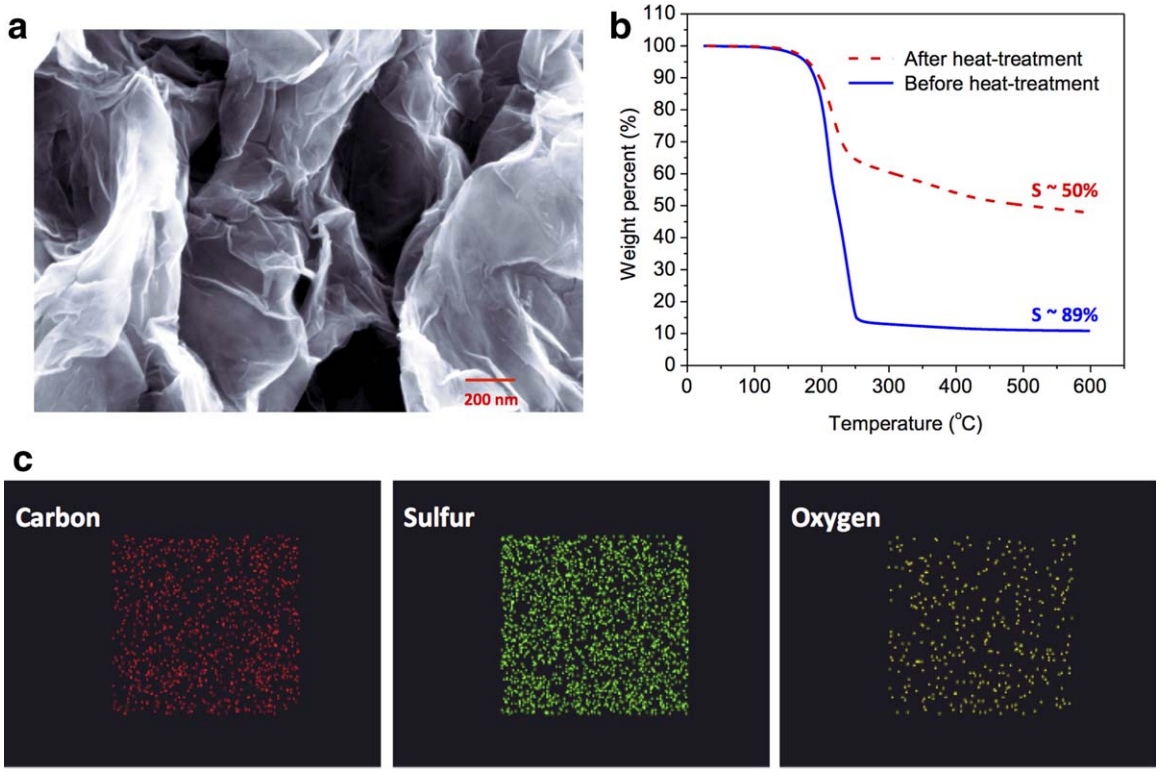

Figure 1. Characterization of S-GO nanocomposite synthesized with 328 mg of CTAB.

(a) Typical morphology observed by scanning electron microscopy (SEM). (b) TGA weight loss of the S-GO composites before and after heat-treatment. (c) Elemental mapping analysis results by energy dispersive x-ray spectroscopy (EDS). [Color figure can be viewed in the online issue, which is available at wileyonlinelibrary.com.]

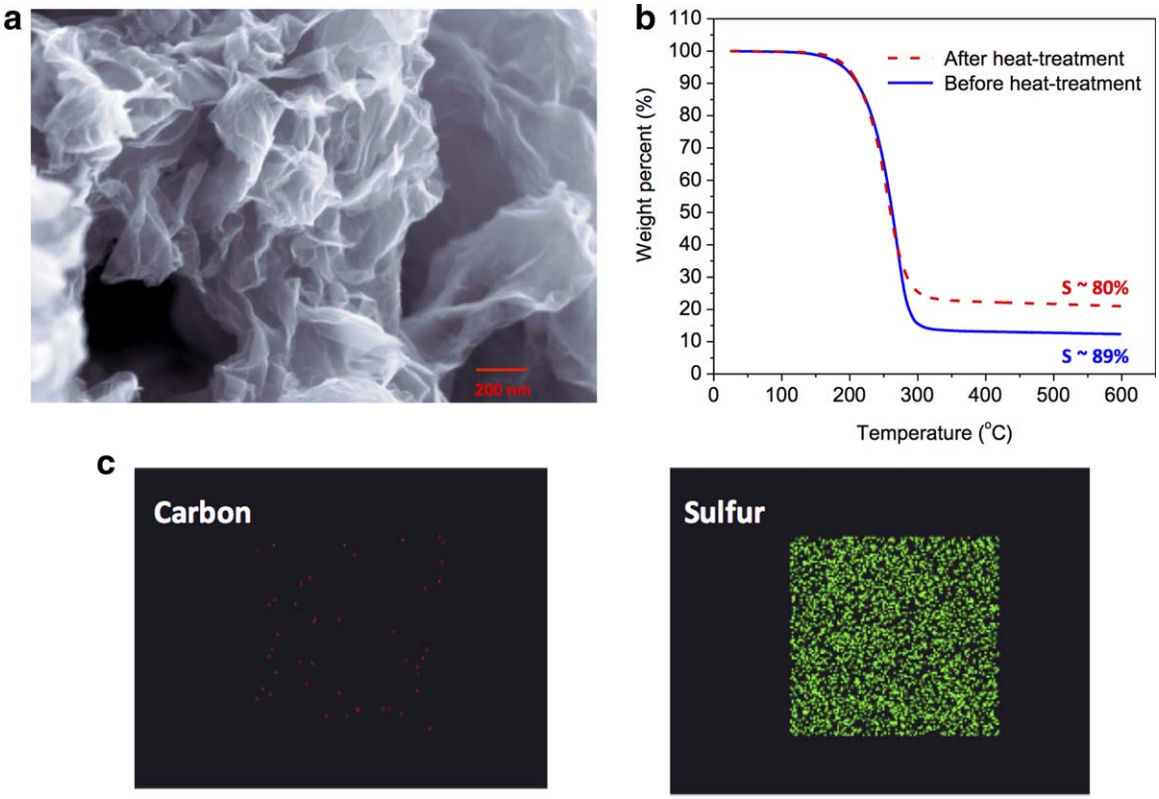

Figure 2. Characterization of S-GO nanocomposite synthesized with 9 mg of CTAB.

(a) Typical morphology observed by SEM. (b) TGA weight loss of the S-GO composites before and after heat-treatment. (c) Elemental mapping analysis results by EDS. [Color figure can be viewed in the online issue, which is available at wileyonlinelibrary.com.]

nanocomposite. These images show that a thin, conformal coating of sulfur was deposited onto the GO.

During the synthesis procedure, CTAB, one kind of cationic surfactant, was introduced in order to modify the surface of the S-GO nanocomposite. In our previous work, Raman spectroscopy showed that in addition to peaks resulting from sulfur and CTAB, a new peak appeared, and can be assigned as a C—S bond, indicating that there is a strong interaction between CTAB and sulfur.[31] Consequently, it was revealed that the amount of CTAB can significantly affect the adsorption extent toward polysulfides, thus affecting sulfur (and capacity) retention. The addition of a larger amount of CTAB led to better cycling performance. It was found that the amount of CTAB affects the sulfur content, especially after heat treatment. TGA curves from CTAB-modified S-GO with different amounts of CTAB (^{9} and 328 mg) introduced during the synthesis are shown in Figures 1b and 2b. The sulfur content of these two samples before heat-treatment were almost identical at ~89 wt %. The sulfur content, however, decreased after heat-treatment due to the evaporation of sulfur. When more CTAB was added, there was more extensive interaction between sulfur and CTAB, resulting in more CTAB in the precipitate before heat treatment. When more CTAB was added, the TGA curves at the higher temperatures are sloped, indicating a more gradual release of sulfur. For example, when 328 mg CTAB was added, the TGA curves (Figure 1b) are not flat at temperatures above 300°C unlike the TGA curves of S-GO synthesized with just 9-mg CTAB (Figure 2b). This indicates that the higher content of CTAB can more significantly retard the loss (evaporation in this case) of sulfur.

As shown in Figures 1c and 2c, energy dispersive x-ray spectroscopy analysis indicated that sulfur was uniformly deposited on the GO. In addition to the elemental sulfur, the other two small peaks were assigned to C and O. Even with 80% sulfur confirmed by TGA analysis, there was a uniform thin sulfur coating, which is critical to achieving high utilization and fast kinetics by providing the reduced diffusion length for lithium within the composites. When the sulfur content is low, C and O peaks with higher intensity appeared (Figure 2c), indicating that the sulfur coating was thinner, which matches well with the TGA analysis results discussed above.

Effect of electrolyte composition on polysulfide shuttle and rate capability

A new electrolyte formulation is needed to further improve cell performance.[33–35] While the main role of the electrolyte in electrochemical cells is to provide a fast transport of ions, in Li/S cells there is a major problem with organic solvent-based electrolytes due to the high solubility of lithium polysulfides.[12] To address this issue, a pyrrolidinium-based ionic liquid ($PYR_{14}TFSI$) has been successfully introduced as an effective solvent to minimize the polysulfide shuttle, as it has lower polysulfide solubility.[36,37]

Figure 3 shows typical discharge and charge curves for Li/S cells with different electrolytes: (a) 1M LiTFSI in $PYR_{14}TFSI$ + PEGDME (1:1 v/v), (b) 1M LiTFSI in $PYR_{14}TFSI$ + PEGDME (1:1 v/v) + 0.1M $LiNO_3$, (c) 1M LiTFSI in $PYR_{14}TFSI$ + DOL + DME (2:1:1 v/v/v)+ 0.1M $LiNO_3$, and (d) 1M LiTFSI in DOL+DME (1:1 v/v). While maintaining the advantage of using the ionic liquid as an effective solvent for minimizing the loss of sulfur as polysulfide, PEGDME, or a mixture of DOL and DME (1:1 v/v) has been added to the ionic liquid to improve the rate capability as they can provide higher conductivity and provide better wettability of the sulfur electrodes. Both PEGDME and DOL/DME worked well with $PYR_{14}TFSI$ and showed good utilization and minimal polysulfide shuttle as evidenced by the charging curves. The addition of 0.1M $LiNO_3$ showed a slightly larger capacity for both discharge and charge as shown in Figure 3a, b.

Generally, $LiNO_3$ is added to further minimize polysulfide shuttle by passivating the lithium metal surface with the formation of a protective film containing lithium nitride.[34,38] $LiNO_3$ is also known to improve coulombic efficiency by decreasing overcharge. The effect of the $LiNO_3$ additive can be seen in Figure 3d. Further, long charging times due to the polysulfide shuttle were found in the DOL/DME electrolyte without any $LiNO_3$. It is important to note that, as shown in Figure3a, an ionic liquid-based electrolyte without $LiNO_3$ did not show the polysulfide shuttle. It can be speculated that the ionic liquid ($PYR_{14}TFSI$) used in this work also forms a passivation layer on the lithium metal surface and it can further provide some protection to the lithium metal electrode and thus cycling performance can be further improved. The composition of this surface layer formed on lithium metal needs further investigation and will be reported elsewhere.

While the performance at low current densities was similar, the rate capability of the Li/S cells using DOL/DME (1:1 v/v) electrolyte was better than with PEGDME as shown in Figure 4. The use of the ionic liquid-based electrolyte with DOL/DME definitely helps to maintain the capacity and coulombic efficiency of the CTAB-modified S-GO nanocomposite electrodes. These results evidently support the conclusion that an ionic liquid-based electrolyte executes well as an effective solvent of stabilizing the sulfur electrode during cell operation, and the addition of DOL/DME and $LiNO_3$ further enhances the rate capability and coulombic efficiency, respectively.

Therefore, 1M LiTFSI in $PYR_{14}TFSI$ + DOL + DME (2:1:1 v/v/v)+ 0.1M $LiNO_3$ was chosen and the performance of Li/S cells with this new formulation of electrolyte is shown in Figures 5–7 and will be discussed in the following sections. However, the composition of this electrolyte needs to be optimized further to achieve longer cycle life with high sulfur loading. In particular, the concentration of $LiNO_3$ needs to be optimized to protect Li metal from direct contact by lithium polysulfides in order to obtain improved cycling performance and coulombic efficiency. Some unique electrode nanostructures reported in the literature showed respectable cycling performance without the addition of ionic liquid in the electrolyte, and it is expected that their performance can be even further enhanced if an ionic liquid is included as established in this study.

In this work, the amount of ionic liquid in the electrolyte has not been optimized. It is worth exploring smaller amounts of ionic liquid because of the high cost. It is noted that ionic liquids are already commercially available and it is the low production volume that has resulted in a relatively high cost. The cost should be significantly lowered when the volume increases. Ionic liquids have been receiving increasing attention and have been investigated worldwide for many different contemporary applications such as powerful solvents, electrolytes for batteries, and pharmaceuticals and it is expected that the manufacturing volume will substantially increase in the near future.

Effect of the sulfur content in the electrodes on specific energy

From a practical perspective, lithium/sulfur cells will need to compete with not only current lithium-ion cells but also

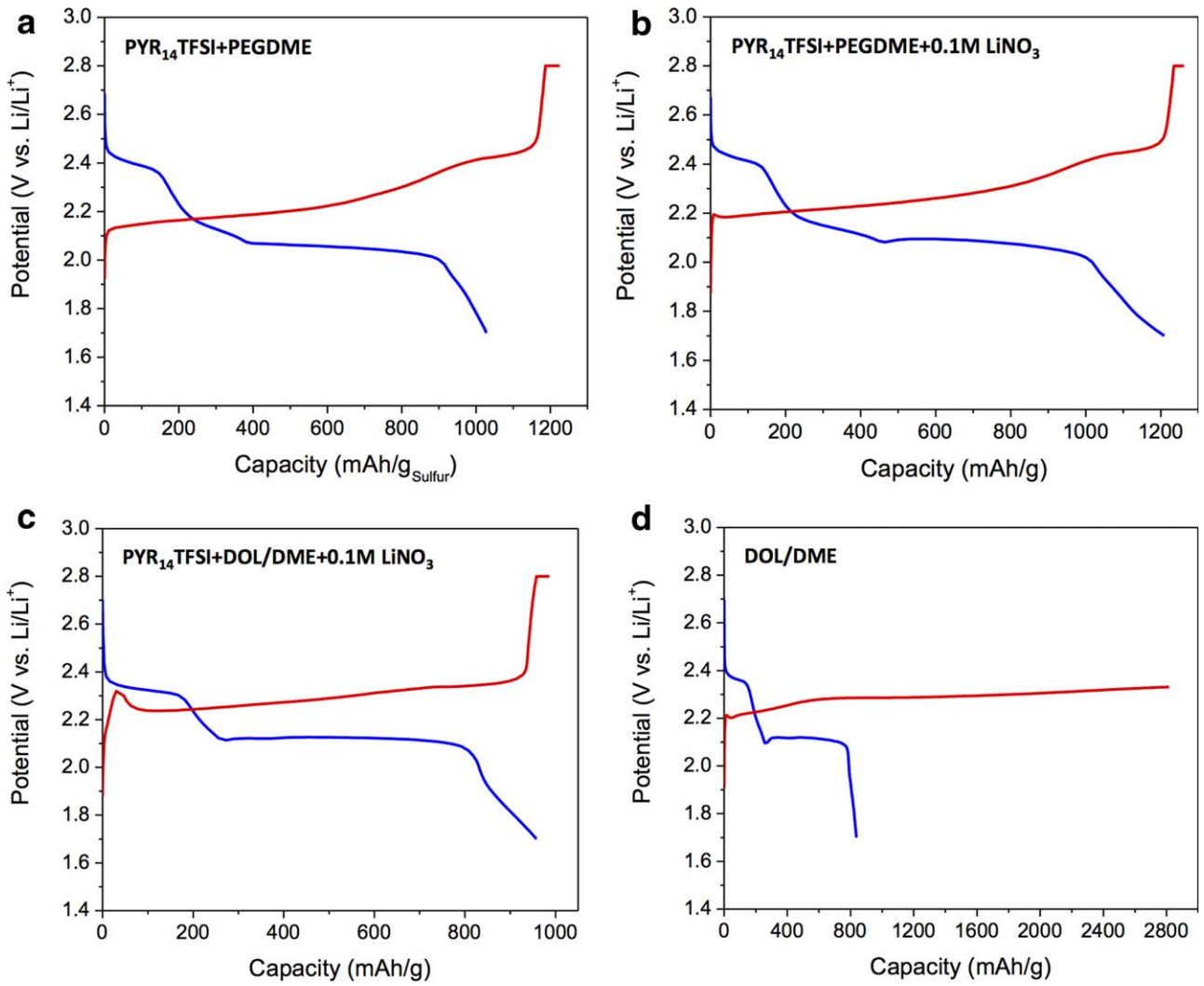

Figure 3. Typical discharge and charge curves for Li/S cells with different electrolytes.

(a) 1M LiTFSI in $PYR_{14}TFSI$ + PEGDME (1:1 v/v), (b) 1M LiTFSI in $PYR_{14}TFSI$ + PEGDME (1:1 v/v) + 0.1M $LiNO_3$, (c) 1M LiTFSI in $PYR_{14}TFSI$ + DOL + DME (2:1:1 v/v/v)+ 0.1M $LiNO_3$, and (d) 1M LiTFSI in DOL+DME (1:1 v/v). These results demonstrate the importance of electrolyte composition (solvents and additive). The CTAB-modified S-GO composite containing 50% S was used as the active material (70% in the composite electrode) and PVDF binder was used. Cells were cycled between 1.7 and 2.8 V at the constant rate of 0.1 C (1 C = 1675 mA/g). The capacity is normalized by the weight of sulfur. [Color figure can be viewed in the online issue, which is available at wileyonlinelibrary.com.]

other energy technologies, such as fuel cells for high specific energy applications.[12] Thus, future investigations should focus more on developing practical cells. To this end, in order to consider these cells for practical applications, their sulfur loading should be significantly increased to improve the overall specific energy while maintaining good cycle life and sulfur utilization. As yet, this issue remains an important challenge.

High cell specific energy levels can be obtained when the loading of sulfur is high, and good utilization is obtained. The specific capacities based on total electrode mass and their demonstrated cycle lives are shown in Figure 5 to illustrate the importance of the sulfur content and loading. While the specific capacity normalized by sulfur is only higher for electrodes fabricated with 50% S, the reverse is true for the actual specific capacity normalized by the electrode mass. In fact, electrodes fabricated with 80% S exhibit higher specific capacity. The specific capacity difference in this work is not great, but can be increased by increasing the content of S-GO from the current 70% to more than 85% or even higher.

Effect of binders in the electrodes on cycle life

In this work, the traditional PVDF binder has been replaced by SBR/CMC to further improve cell performance. The binder plays an important role in prolonging the cycle life of lithium cells, especially for electrode materials that involve large volume changes during cell cycling.[39–41] The important requirements of a good binder in Li/S cells include: (1) good adhesion with electrode materials, (2) the ability to construct a good electronically conductive network structure between sulfur and conductive carbon, and (3) maintenance of the mechanical robustness of the electrode during cycling.[12] For lithium/sulfur cells, among these requirements, the ability to maintain the structural integrity of an electrode is very important as an approximate 78% volume change is involved.

In this respect, elastomeric binders can be a good alternative to PVDF, which is conventionally used in cathodes for lithium-ion cells. Elastomeric rubbery materials are both elastic and viscous, and thus have been commonly used as shock or vibration dampers. Elastomeric materials exhibit low elastic

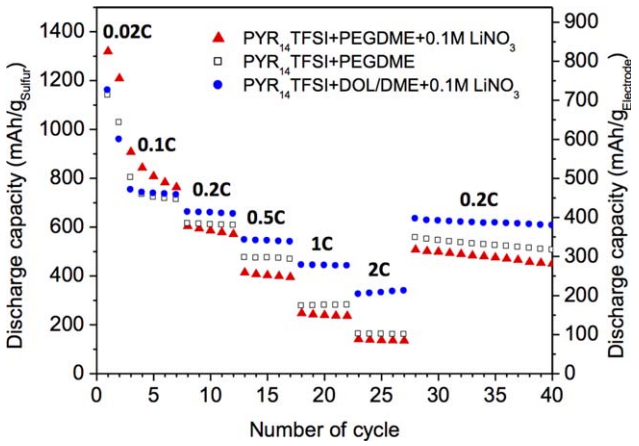

Figure 4. Rate capability of the Li/S cells with different electrolytes.

(a) 1M LiTFSI in $PYR_{14}TFSI$ + PEGDME (1:1 v/v), (b) 1M LiTFSI in $PYR_{14}TFSI$ + PEGDME (1:1 v/v) + 0.1M $LiNO_3$, (c) 1M LiTFSI in $PYR_{14}TFSI$ + DOL + DME (2:1:1 v/v/v)+ 0.1M $LiNO_3$. These results demonstrate the effectiveness of DOL/DME solvent in improving the rate capability of Li/S cells. The CTAB-modified S-GO composite containing 50% S was used as the active material and PVDF binder was used. The cells were cycled between 1.7 and 2.8 V at different C-rates (1 C = 1675 mA/g). The capacity is normalized by the weight of sulfur. [Color figure can be viewed in the online issue, which is available at wileyonlinelibrary.com.]

modulus and are able to withstand a large deformation as much as 1000%. SBR is one type of elastomeric material and its elongation can be as much as 250–700% while the elongation of PVDF is only 20–25%. The Young's modulus of SBR is 2–10 MPa, while PVDF's Young's modulus is 2000–2900 MPa, which points out that PVDF is much stiffer than SBR.

Cycling tests were performed with two sulfur electrodes made with two different binders as shown in Figure 6. The PVDF binder-based electrode showed a decrease in capacity in the beginning of the cycling test due to mechanical degradation. In contrast, the SBR-based electrode showed very stable cycling performance under the same conditions, indicating the important role of the elastomeric binder. The electrochemical impedance spectra of the two electrodes were also measured and compared after 100 cycles of operation. The SBR-based electrode showed much lower charge transfer impedance, representing that the elastomeric binder helps sustain the structural integrity of the sulfur electrode during cycling.

A sulfur electrode made with an elastomeric binder showed good cycling performance at 1 C (1 C = 1675 mA/g of sulfur) and 0.25 C for discharge and charge, respectively. The cycling test was then continued up to 800 cycles as shown in Figure 7. To check the specific capacity that can be obtained at a lower C rate, cells were checked periodically during the long-term cycling test and the discharge and charge capacity were measured using 0.05 C. Even after 800 cycles, the discharge capacity was about 787 mAh/g of sulfur at 0.05 C, which corresponds to ~441 mAh/g of electrode mixture, which leads to 0.47 mAh/cm^2 of electrode. The discharge capacity, however, continued to fade with a low capacity decay rate (0.062% per cycle at 1 C), but the shuttle effect (diffusion back and forth of lithium polysulfides) has been effectively reduced in this study, which is evidenced by the very small overcharges at the low discharge/charge rate (0.05 C) after long-term cycling tests and high coulombic efficiency (e.g., 95.9% after 800 cycles).

Conclusions

Although lithium/sulfur cells have received much attention, the realization of this novel cell chemistries' potential as a commercial product has yet to be successful mostly due to short cycle life. There are three main degradation mechanisms that can lead to capacity fading. These include: (1) the mechanical degradation of electrodes due to volume change (~76%), (2) the dissolution of sulfur (loss as polysulfides), and (3) the polysulfide shuttle (movement of polysulfides between anode and cathode). Although these issues have not been entirely eliminated in this study, we have significantly improved cycling performance by minimizing capacity loss, and have achieved 800 cycles using a CTAB-modified sulfur-GO (to alleviate the loss of sulfur from the electrode by augmenting the absorption capabilities of the active material), using an elastomeric binder (to lessen mechanical degradation), and

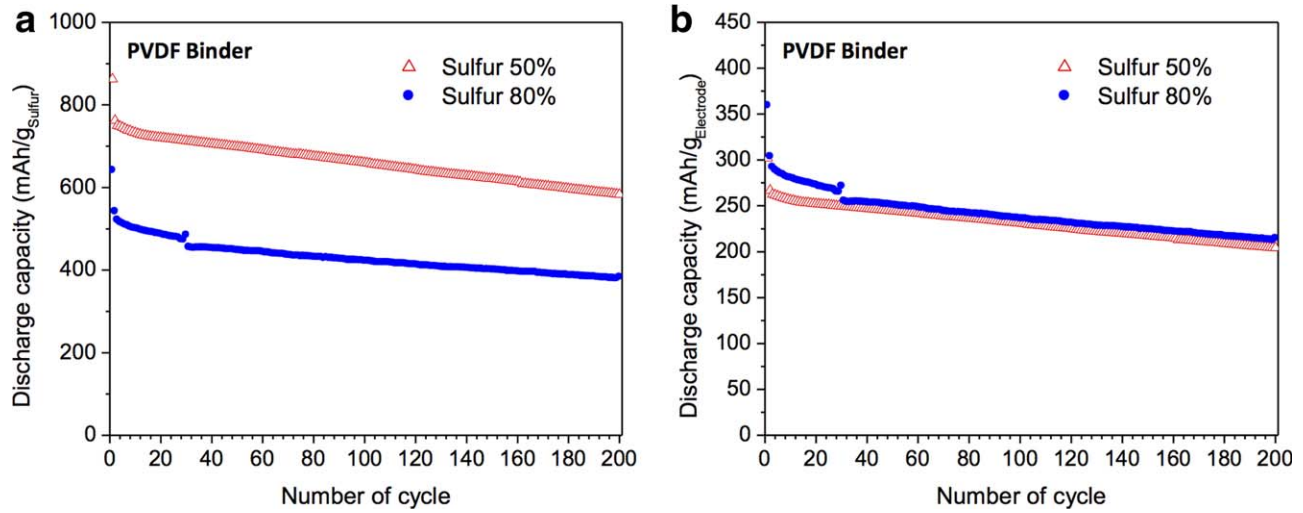

Figure 5. The specific capacities of Li/S cells normalized by (a) sulfur and (b) total electrode mass as a function of cycle number.

The CTAB-modified S-GO composite contained different sulfur loadings (50 and 80% S) and PVDF binder was used. [Color figure can be viewed in the online issue, which is available at wileyonlinelibrary.com.]

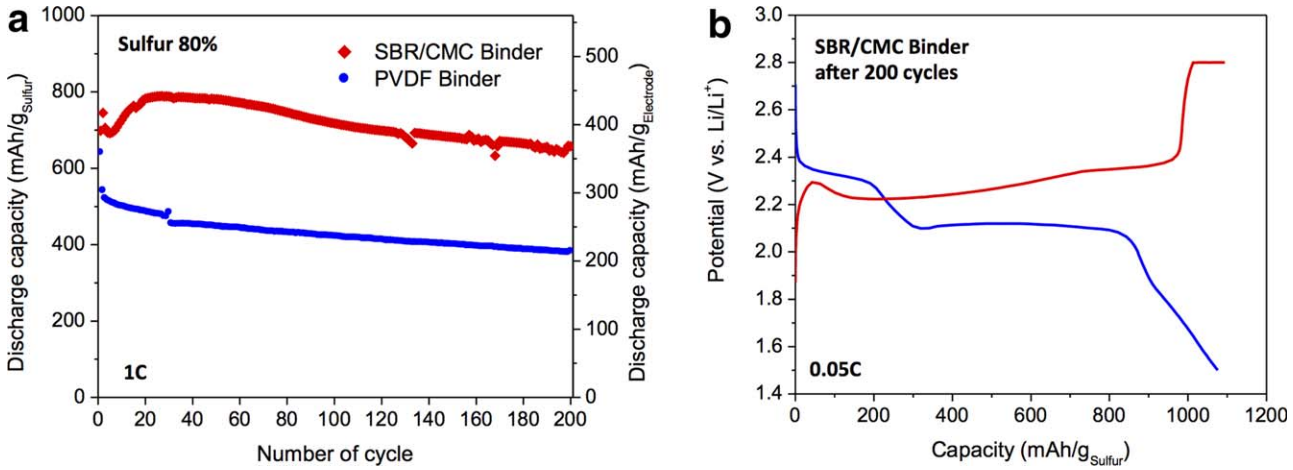

Figure 6. (a) Cycling performance of Li/S cells fabricated with different binders (PVDF and SBR/CMC) obtained at 1 C/0.25 C discharge/charge. (b) Voltage profiles obtained at 0.05 C of Li/S cells fabricated with SBR/CMC binder after 200 cycles at 1 C/0.25 C discharge/charge. The CTAB-modified S-GO composite containing 80% S was used as the active material (70% of the composite in the electrode). LiTFSI (1M) in $PYR_{14}TFSI$/DOL/DME mixture (2:1:1 by volume) with 0.1M $LiNO_3$ was used as the electrolyte (total 60 μL). The cells were cycled between 1.5 and 2.8 V. The capacity is normalized by the weight of sulfur.

[Color figure can be viewed in the online issue, which is available at wileyonlinelibrary.com.]

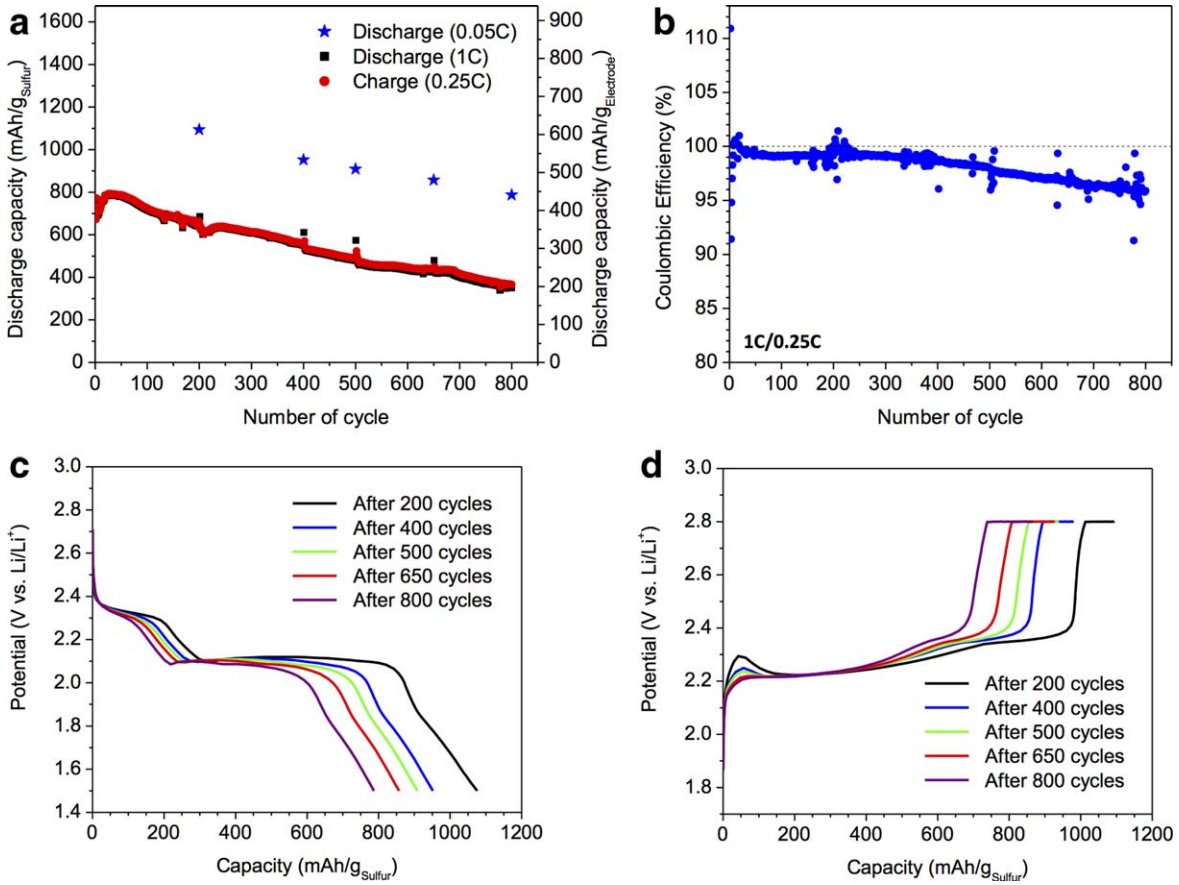

Figure 7. (a) Long-term cycling test results and (b) coulombic efficiency of the Li/S cell. (c) Discharge and (d) charge profiles of Li/S cells at different cycle numbers. The CTAB-modified S-GO composite contained 80% S and elastomeric SBR/CMC binder was used. LiTFSI (1M) in $PYR_{14}TFSI$/DOL/DME mixture (2:1:1 by volume) with 0.1M $LiNO_3$ was used as the electrolyte (total 60 μL). The cells were cycled between 1.5 and 2.8 V. The capacity is normalized by the weight of sulfur.

[Color figure can be viewed in the online issue, which is available at wileyonlinelibrary.com.]

using an ionic liquid based electrolyte ($PYR_{14}TFSI$/DOL/DME mixture, 2:1:1 by volume) as an effective solvent (to minimize the dissolution of sulfur and polysulfide shuttle). Another noteworthy attribute of this study is that the lithium metal electrode exhibited over 800 cycles with no cell shorting triggered by lithium dendrites, when used with ionic liquid-based electrolytes, which may allow for the removal of graphite or silicon as a negative electrode in current lithium-ion cells. We recognize that additional work is still needed to commercialize this technology, especially for electric vehicle applications. As an example, we are now increasing sulfur loading and sulfur content, while maintaining the high utilization and long cycle life demonstrated in this work.

Acknowledgments

This work was supported by the University of California, Office of The President, UC Proof of Concept award No. 12PC247581, and an Innovation Grant, from Lawrence Berkeley National Laboratory. Work at the Molecular Foundry was supported by the Office of Science, Office of Basic Energy Sciences, of the U.S. Department of Energy under Contract No. DE-AC02-05CH11231. The authors thank Tev Kuykendall for his support of the work conducted at the Molecular Foundry, LBNL.

Literature Cited

1. Armand M, Tarascon JM. Building better batteries. *Nature*. 2008; 451(7179):652–657.
2. Goodenough JB, Park KS. The Li-ion rechargeable battery: a perspective. *J Am Chem Soc*. 2013;135(4):1167–1176.
3. Song M-K, Park S, Alamgir FM, Cho J, Liu M. Nanostructured electrodes for lithium-ion and lithium-air batteries: the latest developments, challenges, and perspectives. *Mater Sci Eng R: Rep*. 2011; 72(11):203–252.
4. Tarascon J-M, Armand M. Issues and challenges facing rechargeable lithium batteries. *Nature*. 2001;414(6861):359–367.
5. Ellis BL, Lee KT, Nazar LF. Positive electrode materials for Li-ion and Li-batteries. *Chem. Mater*. 2010;22(3):691–714.
6. Ohzuku T, Brodd RJ. An overview of positive-electrode materials for advanced lithium-ion batteries. *J. Power Sources*. 2007;174(2):449–456.
7. Doug T. *FreedomCAR Program R&D on Energy Storage Systems*. Washington, DC: Office of Basic Energy Sciences, U.S. Department of Energy; 2003.
8. Li W, Zheng G, Yang Y, Seh ZW, Liu N, Cui Y. High-performance hollow sulfur nanostructured battery cathode through a scalable, room temperature, one-step, bottom-up approach. *Proc Natl Acad Sci USA*. 2013;110(18):7148–7153.
9. Nazar LF, Cuisinier M, Pang Q. Lithium-sulfur batteries. *MRS Bull*. 2014;39(05):436–442.
10. Manthiram A, Fu Y, Chung S-H, Zu C, Su Y-S. Rechargeable lithium–sulfur batteries. *Chem Rev*. 2014;114(23):11751–11787.
11. Bruce PG, Freunberger SA, Hardwick LJ, Tarascon J-M. Li-O2 and Li-S batteries with high energy storage. *Nat. Mater*. 2012;11(1):19–29.
12. Song M-K, Cairns EJ, Zhang Y. Lithium/sulfur batteries with high specific energy: old challenges and new opportunities. *Nanoscale*. 2013;5(6):2186–2204.
13. Ji XL, Nazar LF. Advances in Li-S batteries. *J Mater Chem*. 2010; 20(44):9821–9826.
14. Manthiram A, Fu Y, Su Y-S. Challenges and prospects of lithium–sulfur batteries. *Acc Chem Res*. 2012;46(5):1125–1134.
15. Yang Y, Zheng G, Cui Y. Nanostructured sulfur cathodes. *Chem Soc Rev*. 2013;42(7):3018–3032.
16. Cai K, Song M-K, Cairns EJ, Zhang Y. Nanostructured Li2S–C composites as cathode material for high-energy lithium/sulfur batteries. *Nano Lett*. 2012;12(12):6474–6479.
17. Yang Y, Yu GH, Cha JJ, Wu H, Vosgueritchian M, Yao Y, Bao Z, Cui Y. Improving the performance of lithium-sulfur batteries by conductive polymer coating. *ACS Nano*. 2011;5(11):9187–9193.
18. Zhang B, Qin X, Li GR, Gao XP. Enhancement of long stability of sulfur cathode by encapsulating sulfur into micropores of carbon spheres. *Energy Environ Sci*. 2010;3(10):1531–1537.
19. Ji X, Evers S, Black R, Nazar LF. Stabilizing lithium-sulphur cathodes using polysulphide reservoirs. *Nat Commun*. 2011;2:325.
20. Guo J, Yang Z, Yu Y, Abruña HcD, Archer LA. Lithium–sulfur battery cathode enabled by lithium–nitrile interaction. *J Am Chem Soc*. 2012;135(2):763–767.
21. Nan C, Lin Z, Liao H, Song M-K, Li Y, Cairns EJ. Durable carbon-coated Li_2S core–shell spheres for high performance lithium/sulfur cells. *J Am Chem Soc*. 2014;136(12):4659–4663.
22. Jung Y, Kim S. New approaches to improve cycle life characteristics of lithium–sulfur cells. *Electrochem Commun*. 2007;9(2):249–254.
23. Xiao L, Cao Y, Xiao J, Schwenzer B, Englehard MH, Saraf LV, Nie Z, Exarhos GJ, Liu J. A soft approach to encapsulate sulfur: polyaniline nanotubes for lithium-sulfur batteries with long cycle life. *Adv Mater*. 2012;24(9):1176–1181.
24. Jayaprakash N, Shen J, Moganty SS, Corona A, Archer LA. Porous hollow carbon@ sulfur composites for high-power lithium–sulfur batteries. *Angew Chem Int Ed*. 2011;123(26):6026–6030.
25. Feng X, Song M-K, Stolte WC, Gardenghi D, Zhang D, Sun X, Zhu J, Cairns EJ, Guo J. Understanding the degradation mechanism of rechargeable lithium/sulfur cells: a comprehensive study of the sulfur-graphene oxide cathode after discharge/charge cycling. *Phys Chem Chem Phys*. 2014;16(32):16931–16940.
26. Li N, Zheng M, Lu H, Hu Z, Shen C, Chang X, Ji G, Cao J, Shi Y. High-rate lithium–sulfur batteries promoted by reduced graphene oxide coating. *Chem Commun*. 2012;48(34):4106–4108.
27. Mikhaylik YV, Akridge JR. Polysulfide shuttle study in the Li/S battery system. *J Electrochem Soc*. 2004;151(11):A1969-A1976.
28. Schuster J, He G, Mandlmeier B, Yim T, Lee KT, Bein T, Nazar L. Spherical ordered mesoporous carbon nanoparticles with high porosity for lithium–sulfur batteries. *Angew Chem Int Ed*. 2012;51(15): 3591–3595.
29. Guo J, Xu Y, Wang C. Sulfur-impregnated disordered carbon nanotubes cathode for lithium–sulfur batteries. *Nano Lett*. 2011;11(10):4288–4294.
30. Xin S, Gu L, Zhao N-H, Yin YX, Zhou L-J, Guo Y-G, Wan L-J. Smaller sulfur molecules promise better lithium–sulfur batteries. *J Am Chem Soc*. 2012;134(45):18510–18513.
31. Song M-K, Zhang Y, Cairns EJ. A long-life, high-rate lithium/sulfur cell: a multifaceted approach to enhancing cell performance. *Nano Lett*. 2013;13(12):5891–5899.
32. Ji L, Rao M, Zheng H, Zhang L, Li Y, Duan W, Guo J, Cairns EJ, Zhang Y. Graphene oxide as a sulfur immobilizer in high performance lithium/sulfur cells. *J Am Chem Soc*. 2011;133(46):18522–18525.
33. Gao J, Lowe MA, Kiya Y, Abruña HcD. Effects of liquid electrolytes on the charge–discharge performance of rechargeable lithium/sulfur batteries: electrochemical and in-situ x-ray absorption spectroscopic studies. *J Phys Chem C*. 2011;115(50):25132–25137.
34. Liang X, Wen Z, Liu Y, Wu M, Jin J, Zhang H, Wu X. Improved cycling performances of lithium sulfur batteries with $LiNO_3$-modified electrolyte. *J Power Sources*. 2011;196(22):9839–9843.
35. Wang W, Wang Y, Huang Y, Huang C, Yu Z, Zhang H, Wang A, Yuan K. The electrochemical performance of lithium–sulfur batteries with LiClO4 DOL/DME electrolyte. *J Appl Electrochem*. 2010; 40(2):321–325.
36. Shin JH, Cairns EJ. Characterization of N-methyl-N-butylpyrrolidinium bis (trifluoromethanesulfonyl) imide-LiTFSI-tetra (ethylene glycol) dimethyl ether mixtures as a Li metal cell electrolyte. *J Electrochem Soc*. 2008;155(5):A368–A373.
37. Shin JH, Cairns EJ. N-Methyl-(n-butyl)pyrrolidinium bis(trifluoromethanesulfonyl)imide-LiTFSI–poly(ethylene glycol) dimethyl ether mixture as a Li/S cell electrolyte. *J Power Sources*. 2008;177(2):537–545.
38. Zhang SS. Role of $LiNO_3$ in rechargeable lithium/sulfur battery. *Electrochim Acta*. 2012;70:344–348.
39. Sun J, Huang Y, Wang W, Yu Z, Wang A, Yuan K. Application of gelatin as a binder for the sulfur cathode in lithium–sulfur batteries. *Electrochim Acta*. 2008;53(24):7084–7088.
40. Cheon S-E, Cho J-H, Ko K-S, Kwon C-W, Chang D-R, Kim H-T, Kim S-W. Structural factors of sulfur cathodes with poly (ethylene oxide) binder for performance of rechargeable lithium sulfur batteries. *J Electrochem Soc*. 2002;149(11):A1437-A1441.
41. Schneider H, Garsuch A, Panchenko A, Gronwald O, Janssen N, Novák P. Influence of different electrode compositions and binder materials on the performance of lithium–sulfur batteries. *J Power Sources*. 2012;205:420–425.

Manuscript received Jan. 24, 2015, and revision received Apr. 13, 2015.